Reconstructed nonlinear dynamics and its applications to complex fluid flows: focus on melt flow extrusion instabilities

Roland Kádár

Chalmers University of Technology, 421 96 Gothenburg, Sweden

ABSTRACT

The method of reconstructed nonlinear dynamics, i.e. the determination of a reconstructed attractor and its characteristics based on experimental data for complex fluid flows, is here outlined. Examples on the analysis of in-situ mechanical pressure fluctuations associated to the supercritical flow of polymer melts during extrusion, i.e. extrusion instabilities, are presented. The in-situ mechanical pressure time series are acquired during the extrusion flow using a high sensitivity extrusion die. The outline focuses on the determination of embedding parameters and the use of Lyapunov metrics to assess the chaotic character of the instabilities observed.

INTRODUCTION

Instabilities and patterns are a common occurrence in nature and dynamical systems of scientific and practical interest.[1] From the rings of Jupiter down to the self assembly of nanofibers into honeycomb structures during electrospinning,[2] to the instabilities developed in the flow between concentric cylinders, see Fig. 1, or cone-plate flow, see Fig. 2, to the appearance of product defects during the polymer melt extrusion flow, these instabilities and patterns can be desired for certain engineering applications, e.g. the mixing process in Taylor-Couette motion, or undesired, e.g. product defects in polymer processing. Regardless, understanding the spatio-temporal dynamics and origins of instability phenomena is of paramount importance for controlling it and to learn about the very nature of these dynamical systems. In the context of materials science, the behavior of the dynamical systems in relation to the microstructure of the materials is of particular importance.

Benchmark problems such as Taylor-Couette flow, Bénard thermal convection, von-Kármán, contraction, etc., flows of pure viscous and viscoelastic polymeric solutions, have been thoroughly studied with regard to their flow stability and nonlinear dynamics. In particular, the Taylor-Couette (TC) flow has received the special attention due to the multiplicity of states observed on the transition from laminar flow to turbulence as evidenced by Fig. 1. In the figure two sets of transitory motions are presented corresponding to a pure viscous fluid flow and a weakly elastic polymer solution. In this case, the stability of the flow can be described by the Reynolds, $Re = \rho v_0 D_0/\eta_0$, and elasticity numbers, $El = Wi/Re$ where $Wi = \lambda_1 \dot{\gamma}$ is the Weissenberg number. It can be ascertained that the TC flow is now mostly understood with respect to the low-dimensional chaos.[3] Questions for pure viscous flows still remain, however, with respect to turbulence.[3] Equally important for practical applications are the flows of complex fluids that exhibit special type of instabilities in the presence of elasticity,[4] e.g. see Fig. 1. Overall, however, less emphasis has been shown, from nonlinear (reconstructed) dynamics point of view, toward polymer processing engineering applications. In particular, melts extrusion is one of the most preferred means of plastics processing in the polymer industry and can be found in a variety of forms throughout current manufacturing operations. One main drawback is that throughput is limited by the appearance of instabilities during polymer melt extrusion. These instabilities represent surface and volume distor-

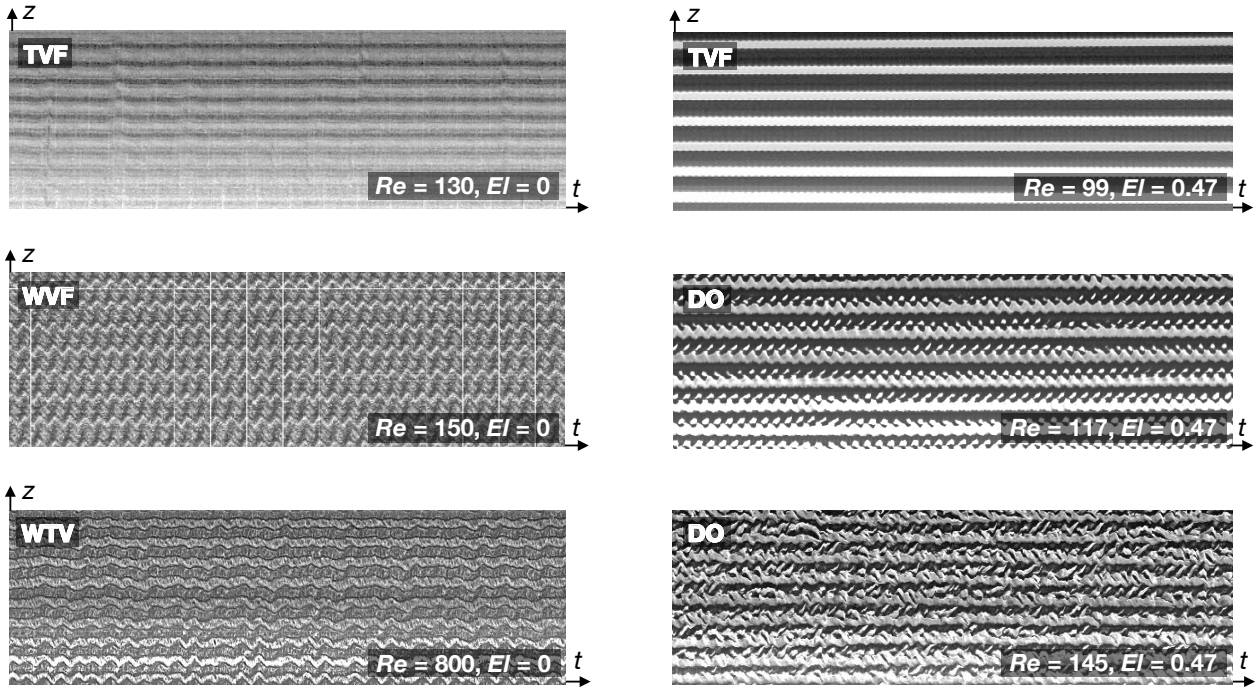

Figure 1. Examples of nonlinear phenomena in the flow between concentric cylinders, where inner cylinder is rotating and the outer one is at rest, i.e. Taylor-Couette flow. The instability types are represented as spatio-temporal diagrams and are: TVF - Taylor vortex flow, WVF - wavy vortex flow, TWV - turbulent wavy vortices and DO - disordered oscillations. The instabilities on the left correspond to the case of a pure viscous fluid whereas those on the right for a weakly elastic polyacrylamide solution.[12,13]

tions of the extrudate that can significantly affect the mechanical performance and appearance of the final products.[5] Comprehensive reviews on the subject of polymer processing instabilities can be found elsewhere.[4,6] With the advent of high sensitivity in situ mechanical pressure instability detection systems in polymer characterization/processing equipments,[7] new means of scientific inquiry are opened. In this context, we provide a new perspective on the extrusion flow instabilities by providing insight into their chaotic character through nonlinear time series analysis. Some of the instability types investigated in the scientific literature, for the extrusion of a linear low density polyethylenes (LLDPE) and low density polyethylenes (LDPE), are presented in Fig. 3 and Fig. 4 (polymer data can be found in ahead Table 1). With increasing control parameter, i.e. the apparent shear rate, $\dot{\gamma}$, the following extrudate states/patterns are distinguished based on their appearance: smooth extrudate, sharkskin, stick-slip, or spurt, and gross melt fracture for LLDPE, whereas in the case of LDPE following smooth extrudate flow instabilities different from those of sharkskin instability appear, followed by a bifurcation to a secondary supercritical regime regime through the addition of a

Figure 2. Nonlinear phenomena observed in a two-phase viscoelastic cone-plate flow. The experiments were performed together with Prof. C. Balan.

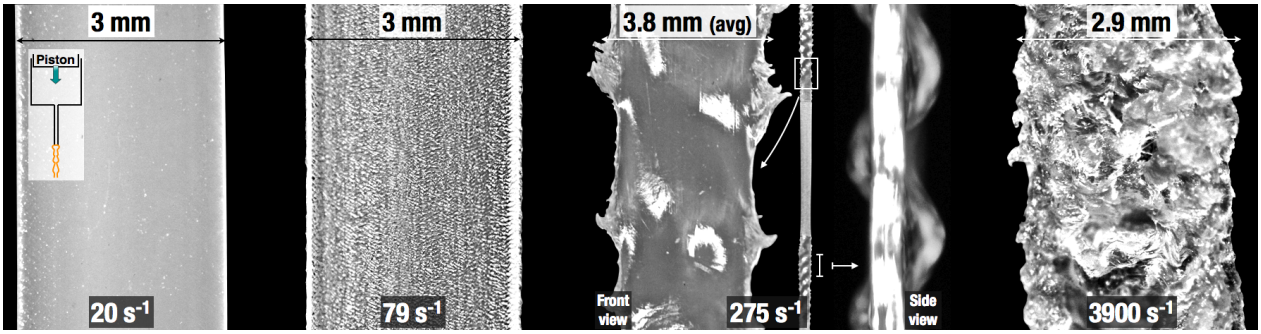

Figure 3. Optical visualization of typical instabilities observed in the extrusion flow of linear/short chain branched polyethylenes.

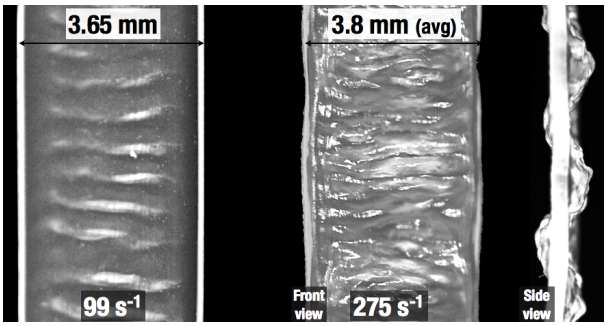

Figure 4. Optical visualization of typical instabilities observed in the extrusion flow of long chain branched polyethylenes.

low frequency component.

In this framework, the method of nonlinear reconstructed dynamics is applied to the polymer melt extrusion stability problem, as an approach to investigate the nature of the dynamical system of complex fluid flows. An overview of the method is shown in Fig. 5. A typical approach in nonlinear dynamics comprises of a given set of equations whose complex solutions comprise an attractor in the phase space. An 'inverse' approach is aimed at creating a reconstructed phase space from experimental time series, even without knowing the original governing equations. In this approach, the reconstructed phase space is defined by some embedding parameters, i.e. delay time, τ, and an embedding dimension, d_E. Various methods are available for the estimation of embedding parameters.[11] Fundamentally, the reconstruction is based on Takens' embedding theorem,[8] that states that the reconstructed phases space is a mapping of the original phase space provided that $d_E \geq 2n+1$, where n is the dimension of the original phase space. In other words, the dynamical system can be reconstructed from experimental time series generated by an unknown system of equations. Thus, in deterministic manner, the state space reconstruction of an unknown nonlinear function F from time series can be represented as:

$$[x(t), x(t-\tau), x(t-2\tau), \ldots x(t-d_E\tau)] \rightarrow F \quad (1)$$

Thus, there exists a topological mapping between the real and reconstructed phase spaces. The topological mapping can be quantified in a number of ways, including by considering the divergence of nearby trajectories, i.e. Lyapunov exponents, among others. The outlined framework can be used to further predict the signal using e.g. artificial neural networks, $F \rightarrow x(t+\tau)$.

EXPERIMENTAL

Two samples of commercial polyethylene with different molecular topologies were used as case study. The first, a low density polyethylene (LDPE; Lupolen 1840 H), is characterized by a random long-chained molecular structure. The second sample is a linear low density polyethylene (LLDPE; Escorene LLN 1201 XV) that differs from the LDPE through its linear molecular structure, molecular mass and its distribution. Their physical properties are listed in Table 1 whereas the rheological properties are shown in Fig. 6. The flow stability of the

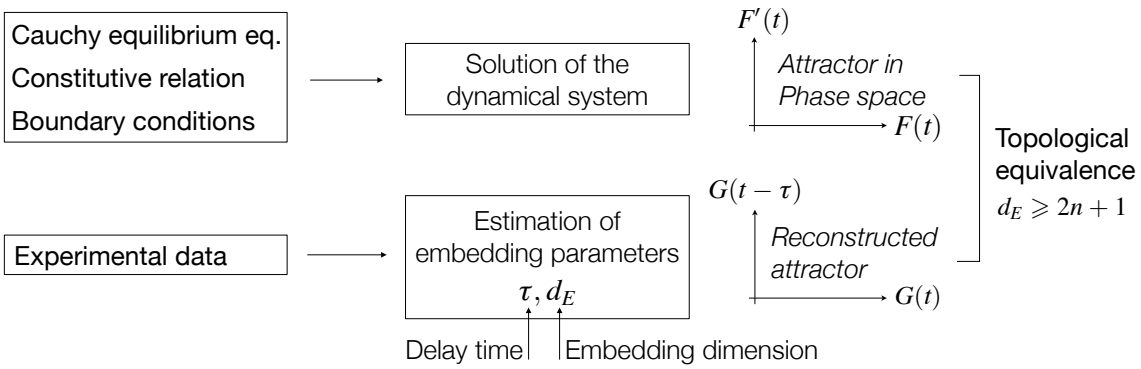

Figure 5. Generic principle of nonlinear reconstructed dynamics.

polymer melts is characterized mainly by the Weissenberg number, $Wi = \lambda_1 \dot{\gamma}$, where λ_1 is the crossing between the dynamic moduli (5-element multimode Maxwell model) and $\dot{\gamma}$ is the apparent shear rate inside the extrusion die.

The experiments were carried out using a Goettfert Rheotester 2000 capillary rheometer, equipped with a custom high-sensitivity instability detection die More details on the experimental system and data acquisition procedures can be found elsewhere.[7,15] The specific routines for nonlinear time series analysis presented in this publication were either implemented in Matlab based on the scientific literature, or the routines in the TISEAN package were utilized or integrated into Matlab codes for optimization.

RESULTS AND DISCUSSION

Examples of representative in-situ mechanical pressure FFT spectra of the LDPE sample are presented in Fig. 7 for subcritical, $Wi < Wi_{cr1}$, and supercritical flows, $Wi_{cr1} < Wi < Wi_{cr2}$. The power spectra exhibits a decay with a slope $s = -1$ (pink noise) at low frequencies for subcritical flows, i.e. due to stochastic processes associated to the data acquisition system (noise). After the onset of instabilities, the power spectra is characterized by low frequency components, as well as higher order

Table 1. Physical properties of the polymers investigated.

	LDPE	LLDPE
$\rho_{25°C}$ / kg/m^3	919	926
T_m / °C	108	125
M_w / kg/mol	256	148
M_w/M_n	15	4.2

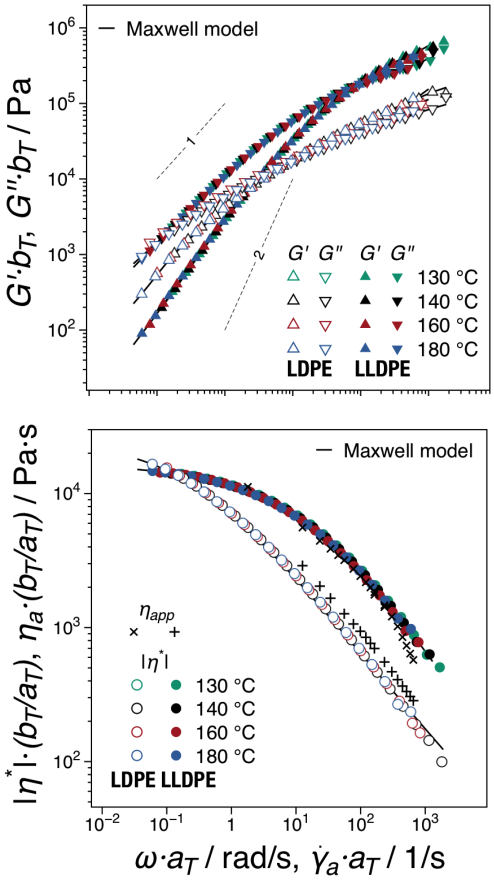

Figure 6. Shear rheology of the tested samples, comprising both rotational as well as capillary rheometry tests (time-temperature superposition and the Cox-Merz rule).

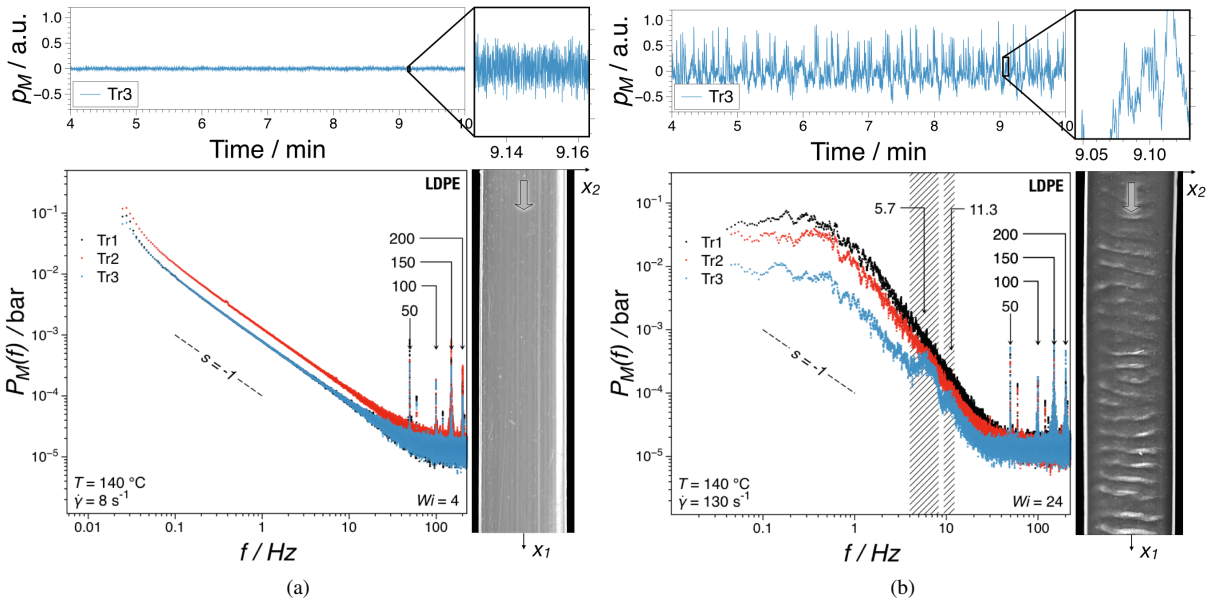

Figure 7. Time series and associated Fourier spectra corresponding to (a) smooth extrudate (subcritical) flow, $Wi < Wi_{cr1}$ and (b) supercritical (extrudates exhibiting instabilities) extrusion flow, $Wi > Wi_{cr1}$ ($< Wi_{cr2}$) for the LDPE sample tested.

characteristic peaks that correspond[15] to the extrudate patterns and their harmonics. A similar behavior is recorded for the LLDPE sample. The existence of these elements in the power spectra can indicate the presence of chaotic behavior.[9]

The characteristic frequencies that correspond to the investigated extrudate patterns, identified based on the steady state FFT of the in-situ mechanical pressure signals are presented in Fig. 8. To assess the correspondence of the in-situ mechanical pressure to the observed extrudate distortions the pressure spectra dynamics was compared to the spectral dynamics associated to spatio-temporal optical imaging analysis.[14] In the investigated parameter range, the LDPE sample tested exhibits two instability types. Following the smooth extrudate regime (e.g. see Fig. 4, similar for both materials), with increasing shear rates small oscillations become visible. This pattern has one characteristic frequency, $\#f_{ch} = 1$, with $f_{ch1} \cong 10^1$ Hz. As Wi is increased a bifurcation is observe, i.e. a new regime with $\#f_{ch} = 2$ is attained. The newly added characteristic frequency is an order of magnitude lower than the main frequency, f_{ch2}, however it is not a subharmonic of f_{ch1}. In the case of LLDPE, typically the instability patterns include the sharkskin instability, $\#f_{ch} = 1$, followed by the stick-slip regime with $\#f_{ch} = 3$, corresponding to the slip frequency, and additional low frequency oscillations as well as sharkskin regions.

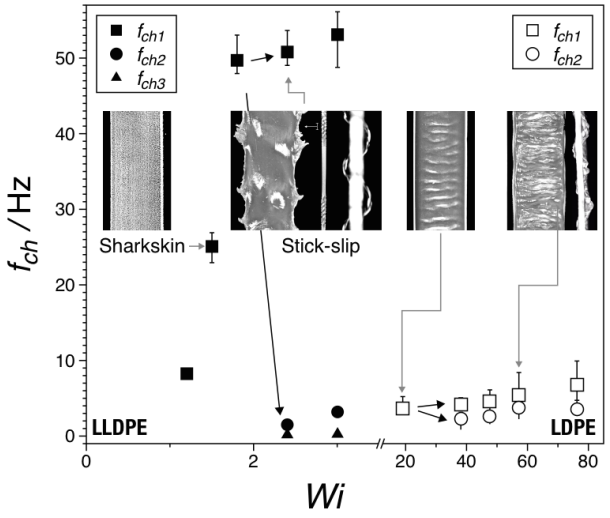

Figure 8. Typical spectral dynamics of the two melt samples analyzed in the investigated range of parameters.

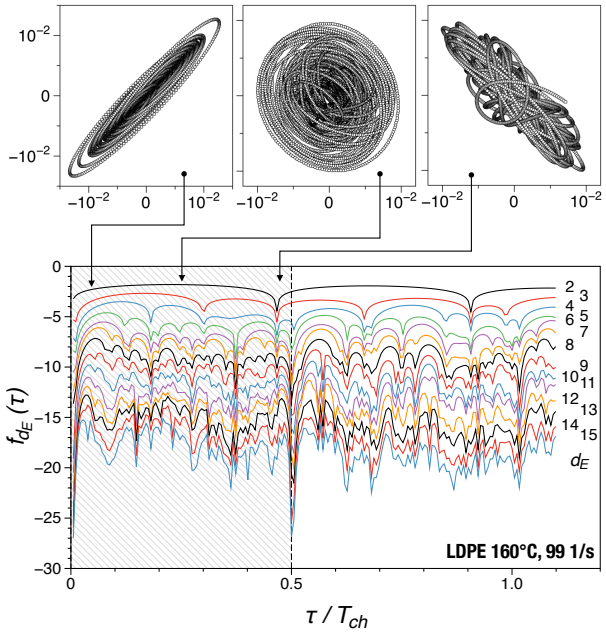

Figure 9. Fill factor, f_{d_E}, as function of normalized embedding time, τ/T_{ch}, for LDPE 140°C, $\dot{\gamma} = 99\ s^{-1}$ ($Wi = 21$), where $T_{ch} = 1/f_{ch1}$.

The embedding parameters, delay time and embedding dimension, τ and d_E, were estimated here using the fill factor, mutual information false nearest neighbor methods.[14] The fill factor algorithm gives a measure of the maximum separation of trajectories in the phase space by looking for the maximal average volume of randomly chosen (hyper)parallelepipeds as function of the delay time.[10] The fill factor is computed as:[10]

$$F_{d_E}(\tau) = \frac{\frac{1}{N_v}\sum_{j=1}^{N_v} V_{d_E, r_0(j)}(\tau)}{[\max(p_M) - \min(p_M)]^{d_E}} \tag{2}$$

where $f_{d_E}(\tau) = \log_{10}[F_{d_E}(\tau)]$ is the fill factor, N_v is the number of control volumes and r_0 is a reference point. Additionally, the the fill factor can be used to estimate the embedding dimension by considering the d_{E_0} at which there is no loss of features in the fill factor for $d_E > d_{E_0}$.[10]

The divergence of trajectories in the reconstructed phase space was considered to determine the existence of Lyapunov exponents. A graphical explanation of the Lyapunov metrics is presented in Fig. 10. Given two points on nearby trajectories on an attractor separated by a distance d_n if and only if after a time Δt the distance increases/decreases exponentially to d_{n+k}, i.e. $d_{n+k} = d_n e^{\lambda \Delta t}$, the Lyapunov exponent can be defined as:

$$\lambda = \frac{1}{\Delta t} \ln\left(\frac{d_{n+k}}{d_n}\right) \tag{3}$$

For experimental data, a number of reference points need to be considered,[11] thereby resulting a so-called maximal Lyapunov exponent, $\lambda_{L_{max}}$. The following scenarios are possible within the framework of maximal Lyapunov exponents: (i) $\lambda_{L_{max}} < 0$ where a stable limit point type of motion is obtained, (ii) $\lambda_{L_{max}} = 0$ where the dynamical system is defined as neutrally stable, i.e. it is composed of self-propagating disturbances, (iii) $\lambda_{L_{max}} \in [0, \infty)$ where the type motion displays a chaotic character and (iv) $\lambda_{L_{max}} = \infty$ that characterizes noise. Different filters and embedding parameters were tested in order to test the validity of their estimation.

The Lyapunov exponents identified are positive for all investigated cases, i.e. all attractors are chaotic. Typically, the radius of the stretching factor was estimated slightly over $\Delta p/100$. The radius was increased until a sufficient number of neighboring points would be found for the expected range of embedding parameters. Having already a possible estimation of the embedding parameters, it remains to be shown that a linear variation in the stretching factor exists, and that it's slope is preserved after a certain critical d_E and for a reasonable range of radii,**?**

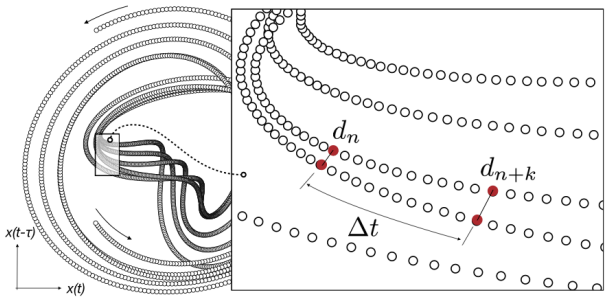

Figure 10. Generic illustration of Lyapunov metrics in a 2D reconstructed phase space.

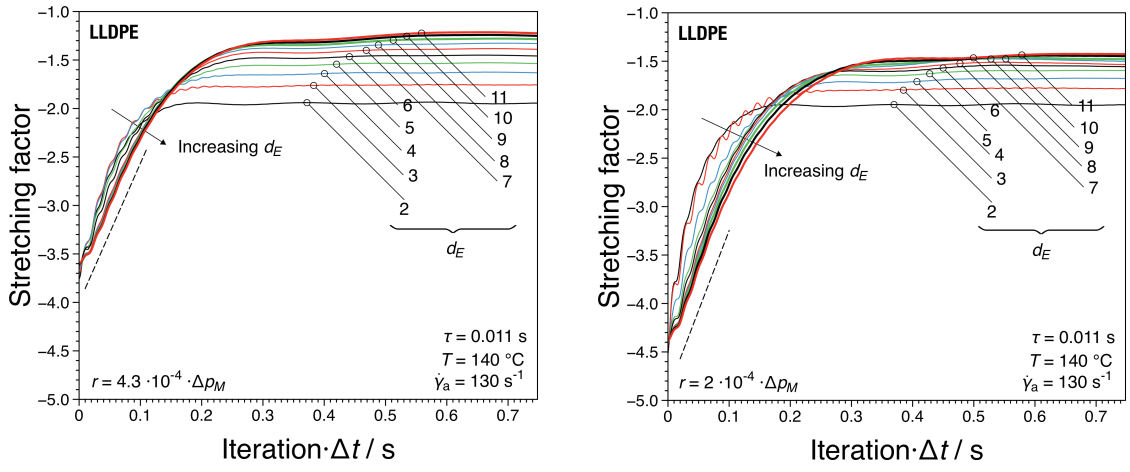

Figure 11. Examples of stretching factor showing the influence of embedding dimension, d_E and radius of the Kantz algorithm, r: (a) $r = 4.3 \cdot 10^{-4} \cdot \Delta p_M$ and (b) $r = 2 \cdot 10^{-4} \cdot \Delta p_M$. The dotted lines represent a linear approximation of the stretching factor for $d_E = 11$. Examples for LLDPE, $T = 140\,^{\circ}\mathrm{C}$, $\dot{\gamma} = 131\ \mathrm{s}^{-1}$ ($Wi = 2.4$).

r in Eq. (4). To compute the largest Lyapunov exponent the Kantz algorithm was used.[11] In the Kantz algorithm, the stretching factor of nearby trajectories is determined as[11]

$$S = \frac{1}{N_r} \sum_{n_0=1}^{N_r} \ln \left(\frac{1}{|u_{x_{n_0}}|} \sum ||d_{x_{n_0} - x_n}|| \right) \qquad (4)$$

where N_r is the number of reference points, $|u_{x_{n_0}}|$ are the neighborhood points within a cloud of radius r relative to the neighborhood points and $||d_{x_{n_0} - x_n}||$ is the Euclidean norm of neighborhood points to the reference point.

Examples of representative stretching factors are shown in Fig. 11, data computed using a constant radius over the embedding dimension range. In both cases, at the maximal d_E investigated, the total number of points with sufficient lump neighbors within the radius r exceeds 2000 data points. The number of reference points used was $N_{ref} = 50,000$. Thus, for $d_E > 8$ there is little change in the linear slope of the stretching factor. Overall, a linear divergence was found typically in the range of $d_E \in [8, 15]$ in accordance with the qualitative observations deduced from computing the fraction of false nearest neighbors. The complete set of determined slopes of stretching factors' linear divergence is presented in Fig. 12. Overall, there is good agreement between the dynamical behavior of $\lambda_{L_{max}}$ and the in situ spectral and spatio-temporal dynamics observed, i.e. $\lambda_{L_{max}}$ is sensitive to the change of extrudate patterns.

SUMMARY AND CONCLUSIONS

For both polymer melt molecular architectures investigated new patterns result from the growth of low frequencies in addition to the main characteristic pattern frequency, whether superimposed or intermittently. In the framework of reconstructed dynamics, embedding parameters were determined based on mainly by considering a maximal separation of trajectories in a delayed representation. In the subsequent reconstructed phase spaces, the polymer melt instabilities investigated obeyed an exponential growth of trajectories in the reconstructed phase space for the recorded extrusion melt flow instabilities, i.e. there exists $d_E > d_{E_0}$ for which a constant linear increase in the stretching factor is recorded, i.e. positive maximal Lyapunov exponents.

ACKNOWLEDGEMENTS

The author is grateful to the financial support of the CNCSIS BG Grant code 349, the DAAD and DFG Grant WI 1911/14-1 for the differ-

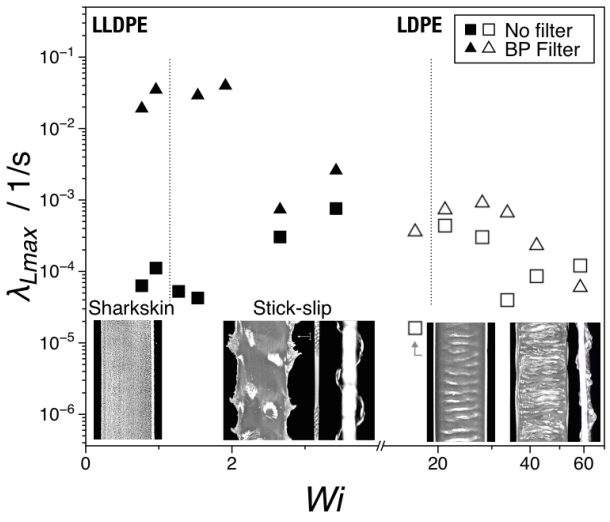

Figure 12. Dynamics of the maximal Lyapunov exponents determined using the Kantz algorithm. Raw mechanical pressure data (no filter applied) and band-pass filtered time series around the relevant frequencies and their higher harmonics (BP Filter) are presented.

ent parts of the experiments presented. Prof. C. Balan, Prof. M. Wilhelm, Prof. S. J. Muller, Prof. M. Kind, Dr. M. Grosso and Prof. R. Dogaru are kindly acknowledged for their help in shaping and developing this work. Dr. D. Ahirwal is acknowledged for fitting the rheological data using the IRIS software.

REFERENCES

1. Cross, M. C. and Hohenberg, P. C. (1993), "Pattern formation outside of equilibrium", *Rev. Mod. Phys.*, **65**, 851.

2. Ahirwal, D., Hebraud, A., Kádár, R., Wilhelm, M. and Schlatter, G. (2013), "From self-assembly of electrospun nanofibers to 3D cm thick hierarchical foams", *Soft Matter*, **9**, 3164-3172.

3. Mullin, T. (2002), "Is chaos relevant to fluid mechanics?", in "Nonlinear Dynamics and Chaos: Where do we go from here?", Hogan, J., Champneys, A. et al.

4. Larson, R. (1992), "Instabilities in viscoelastic flows", *Rheol. Acta*, **31**, 213–263.

5. Denn, M. (2001), "Extrusion Instabilities And Wall Slip", *Ann. Rev. Fluid Mech.*, **33**, 265-287.

6. Denn, M. M. (2004), "Fifty years of non-Newtonian fluid dynamics", *AIChE J.*, **50**, 2335 - 2345.

7. Palza, H., Naue, I. F. C. and Wilhelm, M. (2009), "In situ Pressure Fluctuations of Polymer Melt Flow Instabilities: Experimental Evidence about their Origin and Dynamics", *Macromol. Rapid Commun.*, **30**, 1799-1804.

8. Takens, F. (1981), "Detecting strange attractors in turbulence", in "Dynamical Systems and Turbulence", Warwick, Rand, D. and Young, L.-S.

9. Schuster, H. G. (1984), "Deterministic Chaos", Physik-Verlag, Weinheim.

10. Buzug, T. and Pfister, G. (1992), "Optimal delay time and embedding dimension for delay-time coordinates by analysis of the global static and local dynamical behavior of strange attractors", *Phys. Rev. A*, **45**, 7073–7084.

11. Kantz, H. and Schreiber, T. (2006), "Nonlinear time series analysis", Cambridge Univ. Press., Cambridge

12. Kádár, R., Balan, C. and Kind, M. (2011), "Inertio-elastic instabilities in Taylor-Couette flow", *Math. Model. in Civil Eng.*, **1-2**, 157-165.

13. Kádár, R. and Balan, C. (2012), "Transient dynamics of the wavy regime in Taylor-Couette geometry", *Eur. J. Mech. B. Fluids*, **31**, 158 - 167.

14. Kádár, R., Naue, I. F. and Wilhelm, M. (2015), "Reconstructed dynamics of in situ mechanical pressure fluctuations during polyethylene melt extrusion flows", *(Manuscript in preparation)*.

15. Naue, I. F. C., Kádár, R. and Wilhelm, M. (2015), "A new high sensitivity system to detect instabilities during the extrusion of polymer melts", *Macromol. Mater. Eng.*, 10.1002/mame.201500148.